On the design of fillet welds made of ultra-high-strength steel

Björk Timo, Ahola Antti, Tuominen Niko

DOI: 10.1007/s40194-018-0624-4

ON THE DESIGN OF FILLET WELDS MADE OF ULTRA-HIGH STRENGTH STEEL

Timo Björk, Antti Ahola, Niko Tuominen
Laboratory of Steel Structures
Lappeenranta University of Technology (LUT)
P.O. Box 20, FIN-53851 Lappeenranta, Finland

ABSTRACT

Current static design approaches for fillet arc welds made of high or ultra-high strength steel (UHSS) do not differ from design of welds made of conventional steels. However, important issues such as potential softening in heat affected zone (HAZ), strength at fusion lines, optimal reinforcement geometry, load capacity changes due to local bending moment and the effect of post weld treatments on the joint strength require careful consideration in order to ensure optimum performance from these steels. This paper reprises results of previous research works and recent findings, and summarizes key aspects of weld design specific to UHSS welds.

Keywords: Static strength; welded joint; fillet welds; throat thickness: ultra-high strength steels

1 INTRODUCTION

Joints are essential components of a structure, in terms of design, fabrication and costs. In structures made of ultra-high strength steel (UHSS) with yield strength over 960 MPa, the joints have an even more important role. Essentially, the current design of welded joints made of high and ultra-high strength steels is similar to their counterparts made of lower steel grades (f_y < 500 MPa). However, some additional features of UHSS welds, mainly related to softening or other metallurgical effects must be considered, such as the strength capacity of non-load-carrying joints, critical failure planes in the weld area, the efficiency of penetration depth and the effect of post weld treatments. In this work, these phenomena are examined and discussed and practical recommendations are made for static design of UHSS welds.

2 MATERIALS

The work investigates an thermomechanical UHSS, S960MC (1.8799) [1]. All tests were carried out for joints made of quenched (Q) UHSS. As a matching filler metal, Böhler Union X96 solid wire (for gas metal arc welding) was used in preparation of the test specimens. The maximum and measured chemical compositions, and nominal and measured mechanical properties of the parent and filler materials are presented in Table 1 and Table 2, respectively.

Table 1. Chemical composition of the studied materials (Fe remainder) [wt.%].

Material	Type	C	Si	Mn	P	S	Cr	Ni	Mo	Cu	Nb	N
S960MC	maximum	0.12	0.25	1.30	0.02	0.01						
(t = 8 mm)	measured	0.097	0.20	1.09	0.008	0.001	1.13	0.38	0.191	0.033	0.001	0.005
Union X96 (Ø1.0 mm)	maximum	0.12	0.8	1.9			0.45	2.35	0.55			

Table 2. Mechanical properties of the studied materials.

Material	Type	Proof strength $R_{p0.2}$ [MPa]	Tensile strength R_m [MPa]	Uniform elongation A_5 [%]	Impact KCV [J] (-40°C)
S960MC	nominal	960	980-1250	7	27
S960MC	measured	1041	1210	11	65
Union X96	typical, undiluted WM	930	980	14	47

3 CAPACITY OF THE WELDED JOINT

3.1 Softening and constraint effects of non-load carrying joints

In current design codes such as Eurocode 3 (EC3) [2, 3], recommendations for the design of fillet welds consider only load carrying joints. However, investigations with ultra-high strength steels have shown that fillet welds can have an effect also on the strength capacity of non-load carrying joints [4]. Basically, the strength of the loaded base plate at weld toe can become critical due to the softening effect in the HAZ. Consequently, the non-load carrying joint can become the weakest component of the structure. Degree and extent of softening depends on the cooling rate which is defined by joint geometry (plate thickness and shape factor of joint), preheat/interpass temperature and heat input, which is controlled mainly by the weld size. In single-pass fusion welding, the throat thickness depends on the heat input roughly according to the following equation [5]:

$$a = \sqrt{\frac{Q}{\zeta}} = \sqrt{\frac{\eta UI}{\zeta v}10^{-3}} \tag{1}$$

where:
a = throat thickness [mm]
Q = heat input [kJ/mm]
η = thermal efficiency of the process [-]
U = arc voltage [V]
I = welding current [A]
v = travel speed [mm/s]
ζ = material coefficient [kJ/mm^3]

Then, the cooling rate can be estimated by means of cooling time $t_{8/5}$, which is based on a simplified calculation model for different joint types. Eq. (2) and Eq. (3) are valid for three-dimensional heat flux and two-dimensional flux cases, respectively [6, 7]:

$$t_{8/5} = \left(6700 - 5 \cdot T_P\right) \cdot Q \left(1/\left(500 - T_P\right) - 1/\left(800 - T_P\right)\right) \cdot F_3 \tag{2}$$

$$t_{8/5} = \left(4300 - 4.3T_P\right) \cdot 10^5 \cdot Q^2 / t^2 \left(1/\left(500 - T_P\right)^2 - 1/\left(800 - T_P\right)^2\right) \cdot F_2 \tag{3}$$

where:
Q = heat input [kJ/mm]
t = plate thickness [mm]
T_p = preheat temperature [°C]
F_3 = shape factor for 3D case [-]
F_2 = shape factor for 2D case [-]

Permissible cooling rate ranges depend on the chemical composition and fabrication process of the UHSS. With the exception of tempered UHSSs, there seems to be no maximum limit for the cooling rate for direct quenched steels. More detailed data regarding the dependency of cooling time ($t_{8/5}$) and strength properties of a joint made of quenched UHSS can be found in ref. [8]. If the cooling rate is very low, a wide softened area forms at the weld toe in the loaded base plate, as illustrated in Fig. 1.

Fig. 1. Failure modes of non-load carrying joints: (a) failure at weld toe due to softening, at 45 degrees through the thickness of the base plate (according to Tresca approach); (b) failure with a double 45-degrees mode; and (c) desired failure mode in the base plate outside the joint at an angle of 30 degrees over the width of the plate.

Large throat thickness relative to plate thickness causes a low cooling rate, and thus, a wide and deep softened area occurs at the weld toe, which can lead to failure near the weld toe. To observe the phenomenon critically, the softened area must extend through the plate thickness. Narrow through-thickness softening, however, does not cause failure in the softened area, because the surrounding base material supports the weakened zone due to the local triaxial stress state at the weld toe. The criticality of the weld toe failure depends on the width of the softened area in the loading direction relative to the plate thickness. Amraei *et al.* [9, 10] studied the softening in UHSS and found that in plane strain conditions, the constraint effect increased the effective yield strength by about 65% and in plane stress conditions the strength increase was about 13%.

A double 45-degree mode of yielding can occur if the width of the softened area is roughly half of the plate thickness, which is the theoretical critical width value for the mechanism shown in Fig. 1b. However, softened zone is typically in the inclined direction through the wall thickness, and definition of the critical width is thus more complicated in practice. Additionally, asymmetry of the joint (T-joint instead of X-joint) inhibits the softening effect. The softening results in the reduction of material strength up to 25%. However, due to the location of plastic deformation only in the softened area, the decrease in deformation capacity is more detrimental. This is because the strain hardening with UHSSs is generally weak and cannot compensate the necking. Consequently, it is important to avoid softening, which is possible by either proper design and/or welding techniques.

The cooling rate can be influenced by the weld design. The load carrying capacity of the weld depends on the weld area $a \cdot l$, but the volume of the weld is $a^2 \cdot l$. Hence, optimization of the joint dimensions can provide a possibility to increase the length of the weld and, simultaneously, decrease the throat thickness also in non-load carrying joints, see Fig. 6 in Section 3.2. Reduction of throat thickness increase the cooling rate and, thus, decreases the softening. Other means of minimizing the softening effects include using multi-pass welding instead of single-pass with larger throat thickness [4]. The use of beam processes such as laser and hybrid-laser welding can also help attain optimal cooling rates and thus minimization of softening and its deleterious effects [11, 12].

A joint with a weld reinforcement has a constraint effect, which can inhibit failure at the weld toe even if softening occurs. The constraint caused by the weld reinforcement supports the weakened joint area and can move the location of potential failure away from the heat-affected zone (HAZ) of the joint. The constraint effect is affected by the stress concentration at the weld toe, which causes a triaxial stress state, and thus, compensates the influence of the softening. This phenomenon was demonstrated by Peltoniemi [13]. Fig. 2 shows the capacities of welded joints with and without attachment. In the N-type of joints, the attached plates and/or weld beads were subsequently machined to remove the constraint effect.

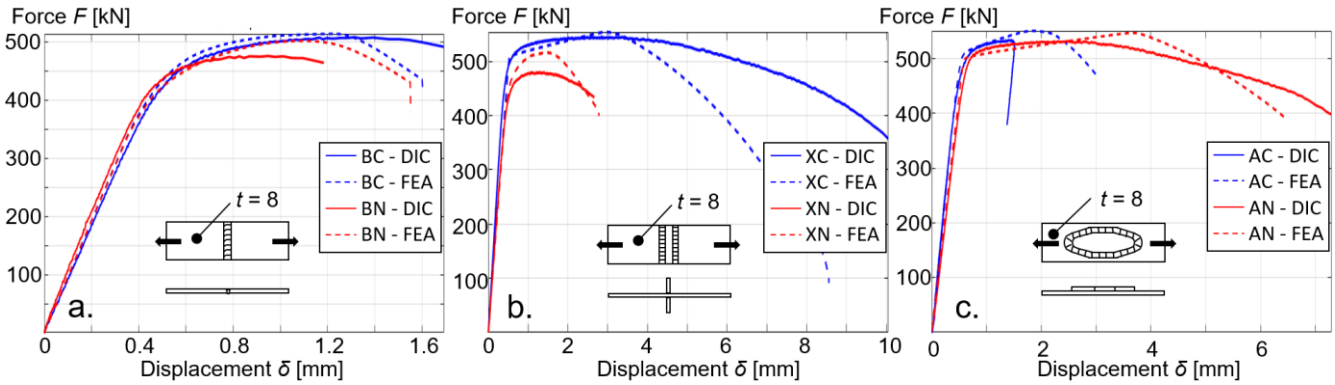

Fig. 2. Effect of constraint on the load carrying and deformation capacities of (a) butt-welded (B), (b) transverse attachment (X) and (c) arrow plate (A) joints with (C) and without (N) constraint effect investigated experimentally (digital image correlation, DIC) and numerically (finite element analysis, FEA) [13].

As can be seen in Fig. 2, a lack of constraint decreases the ultimate load and deformation capacity of the joint. Consequently, high heat input without geometrical constraint can be considered a worst case, and fillet welded joints have a higher ultimate capacity than butt-welded joints for an identical degree of softening. Practical applications that involve softening without any constraint effect include heat treatments without welding, such as bending and straightening by means of local heat. Such treatments should thus be avoided in regions where high strength capacity is needed. If the softened area is wide and extends through the plate thickness, the constraint cannot prevent failure at the weld toe, as illustrated in Fig. 1a and 1b. In the quenched and tempered (QT) UHSS joints, the softened area is far from weld toe than in quenched UHSSs [14], and the constraint effect might not necessarily compensate the softening. However, the more detailed discussion on the constraint effect and failure mode in joints made of QT UHSS lies beyond the scope of this study.

When the failure occurs outside the joint, the critical plane is at an angle of 30 degrees, as shown by Björk *et al*. [15]. The ultimate load capacity based on the critical plane theory must be less than the capacity based on conventional cross section area (principal stress mode), and can be written [15]:

$$F_u = 0.94\frac{btf_y}{\gamma_{M0}}, \tag{4}$$

where:
F_u = ultimate load capacity
b= width of the plate
t = plate thickness
f_y = yield strength
γ_{M0} = partial safety factor for resistance of cross sections

The practical result from this observation is that it is not reasonable to design inclined welds within 0…60 degrees to direction of applied load since the load carrying capacity of the structure does not increase but rather decreases, and furthermore, the weld design causes extra welding cost and longer lead times.

If the strength capacity of the welds in the load carrying joint is higher than the capacity provided by the base material at the weld toe or the parent material, the joint behaves like the non-load carrying joints described previously. However, the stress concentration at the weld toe is greater in load carrying joints and, thus, the constraint effect is wider and greater, too.

3.2 Capacity of load carrying joints

Current design codes assume that rupture of the weld occurs in a plane corresponding to the throat thickness. In the case of an idealized fillet weld with flank angles of 45 degrees, this leads to a failure angle of α = 45 degrees. Consequently, the ultimate load carrying capacity of fillet welds made of UHSS can be calculated based on the stress component (σ, τ) method according to EN 1993-1-8 [2]. For a symmetric fillet weld, the throat thickness can be calculated as follows:

$$a = \frac{\gamma_{M2}\beta_w t}{2 f_u}\sqrt{2\sigma^2 + 3\tau^2}\,, \tag{5}$$

where:
γ_{M2} = partial safety factor for resistance of cross sections in tension to fracture
$ß_w$ = correlation factor
t = plate thickness of loaded component
f_u = ultimate strength of weaker component joined
σ = normal stress in the adjacent plate
τ = shear stress in the adjacent plate

As mentioned earlier in Section 2, matching filler materials are available for S960 steel grades. A large number of tests have been carried out in [4] to investigate the validity of Eq. (5) for S960 grade steel. Such study of load carrying fillet welds faces the problem of being based on a theoretically pure fillet weld: there should be good weld penetration everywhere except at the root, which is difficult to control exactly using welding parameters. To overcome this problem, an infusible thin strip of tungsten was used in the root to establish a perfect root geometry, see Fig. 3a. Naturally, normal penetration as seen in Fig. 3b, can be taken into account in calculations afterwards by measuring the effective throat thickness from the fractured surface. In the case of existing bending moment, however, both effective throat thickness and location of weld have an influence on section modulus and thus, on joint capacity. If penetration and bending loading are included in tests, a precisely planned test program and joint geometry are required. Additionally, other materials than tungsten were investigated, but they caused porosity in the weld and tungsten proved to be the most appropriate material for this purpose.

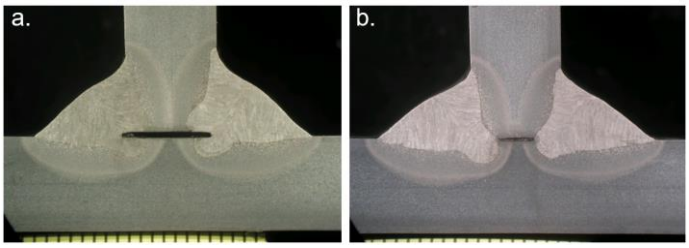

Fig. 3. (a) Use of a tungsten at the root to create a theoretically perfect fillet weld without lack of penetration and (b) a normal penetrated weld without tungsten.

The critical failure plane of fillet welds can be calculated in the general loading case according to von Mises theory. If we assume a symmetric fillet weld as illustrated in Fig. 4, the sufficient leg length can be defined according to the model presented by Penttilä [16]:

$$k_1 \geq \left(\frac{\sin\alpha}{\tan\alpha} + \cos\alpha\right)\sqrt{\sin^2\alpha + 3\cos^2\alpha}\,\frac{\beta_w \gamma_{M2} F_w}{l\ f_u} \tag{6}$$

where l = length of weld and the other symbols are as presented in Eq. (5) or given in Fig. 4b. The highest von Mises stress occurs in the critical plane, which is located at the angle α and can be found by the derivation $dk_1/d\alpha = 0$ giving:

$$\tan\theta \cdot \tan^3\alpha + \tan^2\alpha + 5\tan\theta \cdot \tan\alpha - 3 = 0 \tag{7}$$

From Eq. (6) and Eq. (7) the leg length can now be defined:

$$k_1 \geq \frac{(\cos 2\alpha + 2)^{3/2}}{\cos 3\alpha + 2\cos\alpha}\,\frac{\beta_w \gamma_{M2} F_w}{l\ f_u} \tag{8}$$

In the case of a symmetric fillet weld, i.e. θ = 45 deg, the critical angle is α = 27 deg. To avoid failure in the weld area, a throat thickness requirement is:

$$a \geq 1.53\,\frac{\beta_w \gamma_{M2} F_w}{l\ f_u} \tag{9}$$

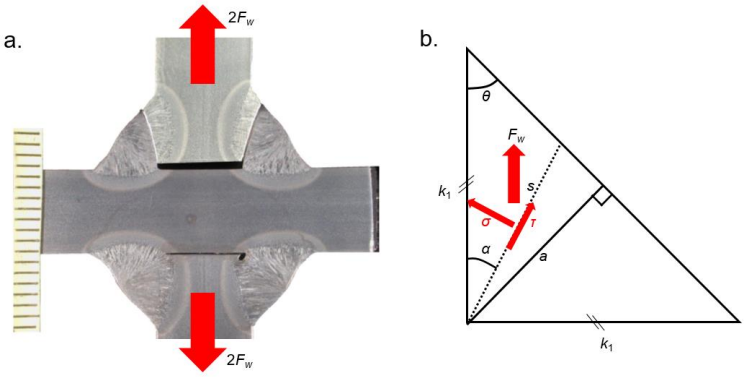

Fig. 4. Critical failure plane of weld: (a) an experimental result and (b) the geometry of a symmetric weld.

Throat thickness calculated by Eq. (9) is only 8% higher than that calculated by the conventional model for a 45-degree failure plane. Actually, the assumption of 45-degree critical plane in the weld is only valid if the joint is subjected to pure shear loading parallel to the weld. The critical plane angle of 27 degrees also agrees quite well with experimental results presented in [17, 18]. Although, the difference in ultimate strength capacity is not significant, it favors the design of asymmetric fillet welds. The design of asymmetric fillet welds is a good practice also in terms of the fatigue design of the joint since it decreases stress concentration at weld toes.

Definition of the critical plane in an asymmetric joint yield to a more complicated mathematical calculation, especially if penetration is included in the model, as illustrated in Fig. 5a. Penttilä [17] investigated this problem and defined the load carrying capacity of a generic weld as:

$$F_w \le \frac{k_1 \, l \, f_u}{\beta_w \gamma_{M2} \tan\theta \cos\varphi \, [\frac{\sin(\alpha'-\varphi)}{\tan(\theta+\varphi)} + \cos(\alpha'-\varphi)]\sqrt{1+2\cos^2(\alpha')}} \tag{10}$$

The area of the weld is:

$$A_w = \frac{{k_1}^2}{2\tan\theta}\left(\frac{\tan\varphi}{\tan\theta}+1\right) \tag{11}$$

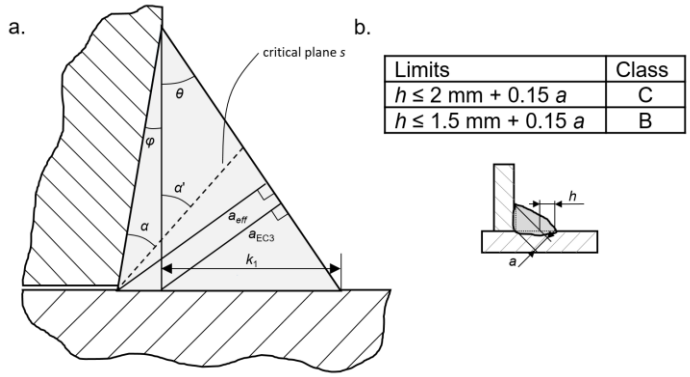

Limits	Class
$h \le 2$ mm + 0.15 a	C
$h \le 1.5$ mm + 0.15 a	B

Fig. 5. (a) Critical plane in an asymmetric weld with penetration and (b) leg length asymmetry limits from ISO 5817 [19].

Optimization of the ultimate strength capacity of the joint with respect to weld area can now be executed numerically based on Eq. (10). It provides a definition of the critical plane α or α' (Fig. 5). Minimization of the weld area not only saves filler material and enhances productivity but also minimizes softening. Typically, the optimal flank angle θ is in the range of 30…40 degrees. However, EN ISO 5817 [19] sets limitations for asymmetric leg lengths given in Fig. 5b, which are based more on trying to avoid a lack of fusion in the weld than consideration of the strength of the joint. Lack of understanding of the beneficial effects of asymmetry on the static and fatigue strength of the joint sometimes leads to asymmetry being considering a quality defect.

The design of the joint geometry has significant role also in static loaded applications when UHSSs are used instead of low or mild steels. As discussed earlier, it can be reasonable to increase the weld length in order to decrease the throat thickness to a size that is optimal for the process used, e.g. a = 4…5 mm for gas metal arc (GMAW) processes. The weld length can be increased by enlarging the plate dimensions or in some cases additional length can be provided by slot welds, as seen in Fig. 6b. Weld design is based on fully plastic conditions over the throat thickness and along the weld perimeter. Consequently, high stress concentrations should be avoided, especially in corner areas, in order to ensure the deformation capacity of the joint. In addition, the overall dimensions and shape of the joint should be considered in the static loading [20].
The design of a UHSS welded joint for static loading requires consideration of the deformation capacity and the avoidance of softening and uneconomical throat thicknesses. It is important to consider the

practical fillet weld limitations, e.g. for cover plates with a thickness of t_c, the maximum (shorter) leg length is roughly t_c - 1 mm. Again, intentional asymmetry improves the performance of the weld, now due to geometrical limitations.

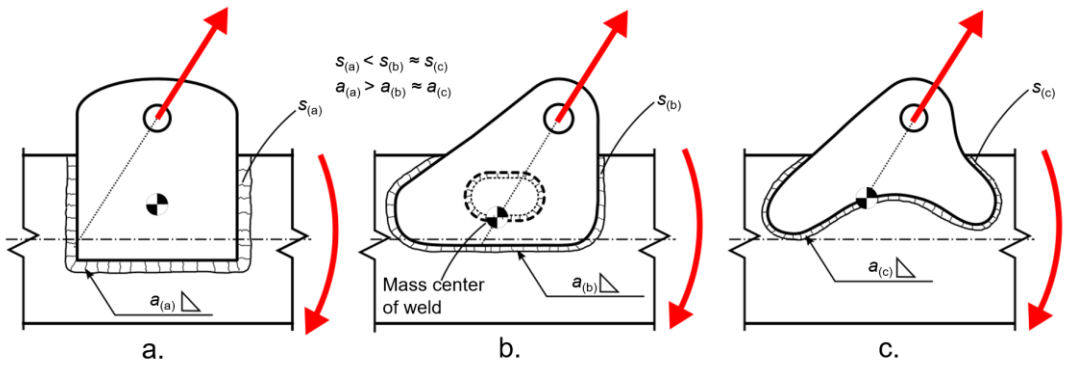

Fig. 6. Example of improving the design of a bracket by taking the deformation capacity, softening effect and economical aspects into account: (a) original basic model, (b) improved geometry with a possible slot for an additional weld and (c) ideal geometry, *s* is perimeter length of weld.

3.3 Fusion line failure

Welded joints made of high strength steels are more prone to fail around fusion lines than welded joints made of low strength (f_y < 500 MPa) steels. Due to the softening and other metallurgical effects, the areas around the fusion lines may be weaker than the adjacent base material and weld metals deposited with strength-matching filler materials, as shown in Fig 7a. If it is assumed that the effective transverse fusion line capacity depend on the throat thickness *a*, rather than leg length $\sqrt{2}\,a$, as illustrated in Fig. 7b, the critical fusion line weakening factor β_{FL} can be defined by setting the load carrying capacity of the weld from Eq. (5) as equal to the strength capacities of the base material at fusion line. The second, parallel fusion line is loaded by pure shear over its length $\sqrt{2}\,a$. Consequently, limits for the weakening factors at transverse ($\beta_{FL,\perp}$) and parallel ($\beta_{FL,\parallel}$) fusion lines are acquired:

$$\beta_{FL,\perp} \le \sqrt{2}\beta_W \text{ and } \beta_{FL,\parallel} \le \frac{2}{\sqrt{3}}\beta_W \tag{12}$$

In the case of S960, the correlation factor is typically β_w= 1 and the weakening factor due to the shear mechanism can thus be equal or less than $2/\sqrt{3}$, which means the reduction in strength due to softening can be only about 14%. This agrees well with experimental results [4, 17] and confirms the validity of this phenomenon. Hardness measurements can be applied to estimate the criticality of this failure mechanism, e.g. using linear dependency of strength properties and hardness [21]. If the fusion line capacity does not meet the design capacity of the joint, an increase in throat thickness is a way to find the balance, which is not, however, an optimal situation. Due to the different requirements for each leg lengths, use of asymmetric welds is, again, a good practice to avoid fusion line failures efficiently. However, there are exceptions, an example of which is described in Section 3.5.

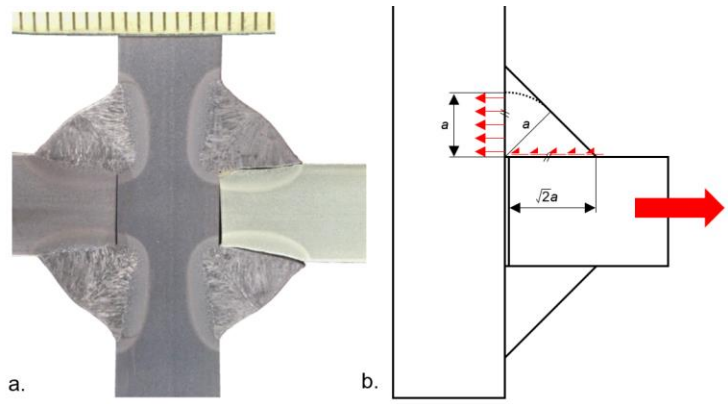

Fig. 7. (a) Fusion line failures in a weld made of UHSS and (b) effective lengths for transverse and parallel fusion line failure paths.

3.4 Increased capacity from penetration

Weld penetration can be exploited to increase ultimate strength capacity of the fillet weld, if the welding process used can produce consistent penetration without interruptions. Penetration improves also the fatigue performance of the joint in terms of both weld toe [22] and weld root [23] failures. Penetration adds to the strength capacity of the joint efficiently because it increases the cross section area of the weld less relative to the increase in the external fillet size, which minimizes the residual stresses and distortion of the structure. The penetration depth can be added to the external throat thickness of fillet weld and a new effective throat thickness a_{eff} (= s, see Section 3.2) can be used for strength analysis. Nevertheless, the increasing penetration depth does not seem to improve proportionally the joint strength. Fig. 8 shows that the average strength of the weld decreases as the degree of penetration increases.

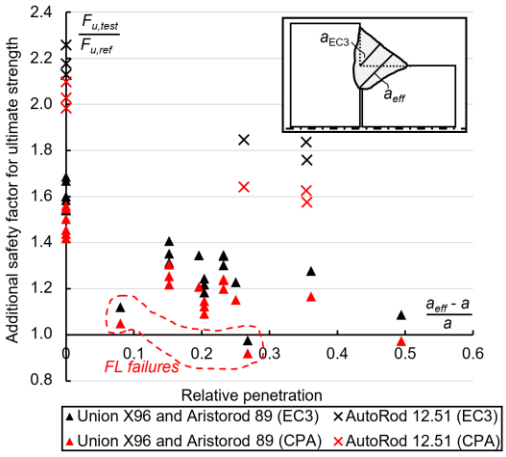

Fig. 8. Ultimate capacity of load carrying joints, as function of weld penetration.

The vertical axis gives the relative strength capacity obtained from the tests referred to the theoretical values calculated applying the EC3 standard, see Eq. (5), and critical plane approach (CPA) and von Mises yield criterion, see Eq. (10). In the case of penetrating weld, the reference capacities are obtained using effective throat thickness, a_{eff}. For S960, the reason for this phenomenon is the increased degree of dilution between the base and filler materials with increasing penetration.

Rasche and Kuhlman [24, 25] have investigated the dilution problem of fillet welds made of UHSS and proposed that both the base and filler materials should be taken into account in evaluation of the reduced ultimate strength $f_{u,red}$, and the weighted value should be calculated as follows [25]:

$$f_{u,red} = 0.25\, f_{u,BM} + 0.75\, f_{u,FM} \tag{13}$$

where:
$f_{u,BM}$ = ultimate strength of base material
$f_{u,FM}$ = ultimate strength of undiluted filler metal

This approach seems to one potential method to consider also the dilution of the penetrated zone.

3.5 Capacity under bending moment

In EC3, there are no design rules for welds subjected to bending moment as this issue is still under investigation [26, 27]. The failure path can occur in the critical plane of the weld as presented in Section 3.2 or along the leg length, depending on the degree of bending and the joint geometry.

However, in many applications, a secondary bending occurs in the weld subjected to tensile load. Fortunately, the bending moment can cause compressive stresses at the root of weld, which is especially the case with tubular joints as illustrated in Fig. 9a. One reason for the good load and deformation capacity found in practice with such joints is the beneficial secondary bending. On the other hand, it is important to recognize also the opposite behavior occurring in joints illustrated in Fig. 9b where both axial loading and secondary bending causes tensile stress at root side, i.e. combined tensile loading. Such joints are typical in box structures.

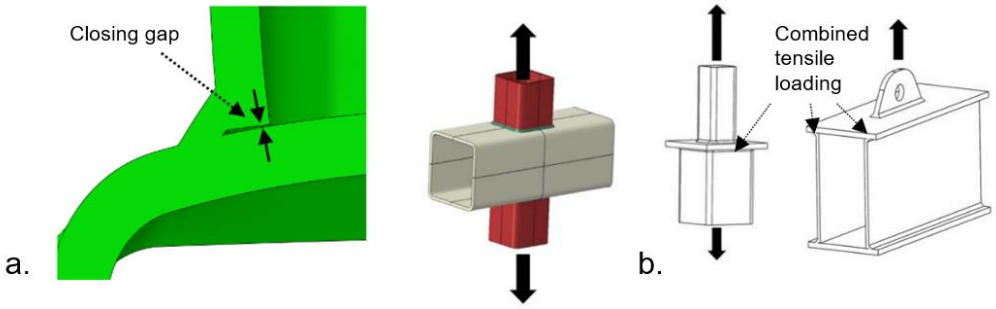

Fig. 9. Joints where welds are subjected to secondary bending moments causing a) compressive stresses in the weld root and b) tensile stresses, respectively.

The EC3 standard [2] does not give unambiguous instructions for consideration of primary or secondary bending stresses in the static design of fillet welds. In general, if a joint has sufficient deformation capacity, the secondary bending stresses, e.g. caused by weld eccentricity, can be neglected. However, this justification is not necessarily valid for welded joints made of UHSS. Therefore, some preliminary tests for fillet and butt welds were carried out [26, 27] in order to produce some design recommendations. These tests showed that the direction of local bending moment has a significant effect on the load capacity of the joint. In the example given in Fig. 10, considering the real throat thicknesses, the strength capacity was about twice as large for the case with bending causing compressive stresses in the root (RC02) than when loading was causing tensile stresses in the root (RC01). The change in the deformation capacity is even higher due to the fact that the weld never failed when the root side was compressed.

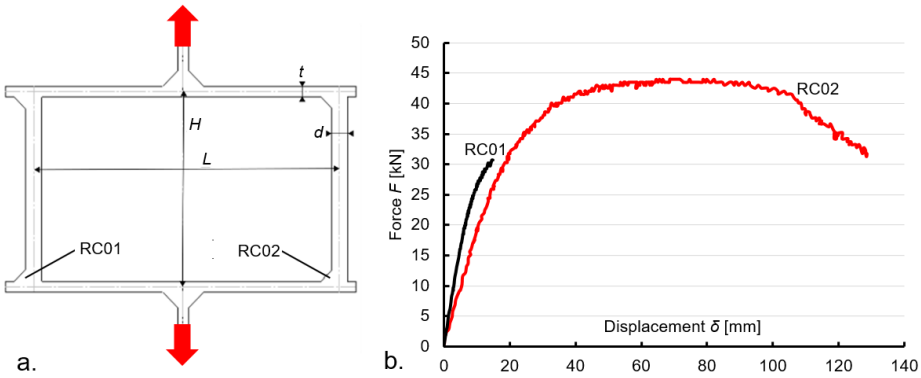

Fig. 10. (a) Test specimens (t = 6 mm, d = 9 mm) and (b) test results.

The load carrying capacity of a welded joint F_W subjected also to secondary bending moment is [26]:

$$F_W = \frac{nabf_u}{\beta_w \sqrt{\left[\cos\alpha + \frac{k(nb+e)}{a}\right]^2 + 3\sin^2\alpha}}, \tag{14}$$

where:
k = 6 for elastic and k = 4 for fully plastic stress distribution, respectively
n = number of load bearing (web) plates
e = eccentricity between the plates and weld
a = throat thickness (in the critical plane and can distinguish from a_{eff})
α = angle between the acting force F and the normal of the critical plane
b = length of the weld (and joint)
β_w = ratio between the ultimate strengths of the base and filler materials
f_u = ultimate strength of the base material

Experimental results [26] show that the elastic approach factor k = 6 must be applied in the case when the root side of the joint is subjected to a combined tensile loading and plastic factor k = 4 can be used, if the root is under compressive loading.

3.6 Post weld improvement methods

Post weld improvement methods are used to improve the fatigue performance of welded joints. However, it is important to know whether post weld treatment has any effect on the ultimate capacity of welded joints made of UHSS. In [28], fillet welds made by GMAW process were post weld treated by burr grinding, TIG dressing, laser dressing and high frequency mechanical impact (HFMI) treatment and the results were compared to the capacities of the as-welded joints. The diagram of the specimens used in the study is shown in Fig. 11.

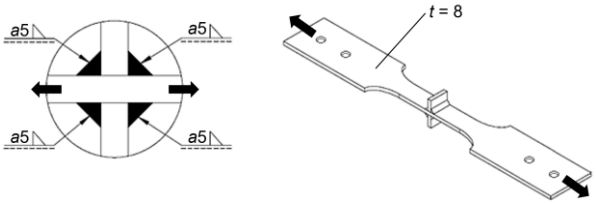

Fig. 11. Test specimens to study the effects of post weld treatment.

Laser dressing is not a very common process and some preliminary tests to establish effect of travel speed and power on weld toe profile were perfomed, the main results of which are shown in Fig. 12. The power of 2 kW and travel speed of laser beam of 0.5 m/min resulted in the best shape of the dressed weld toe, see Fig. 12c, and consequently, those parameters were chosen for post weld treatment of test specimens

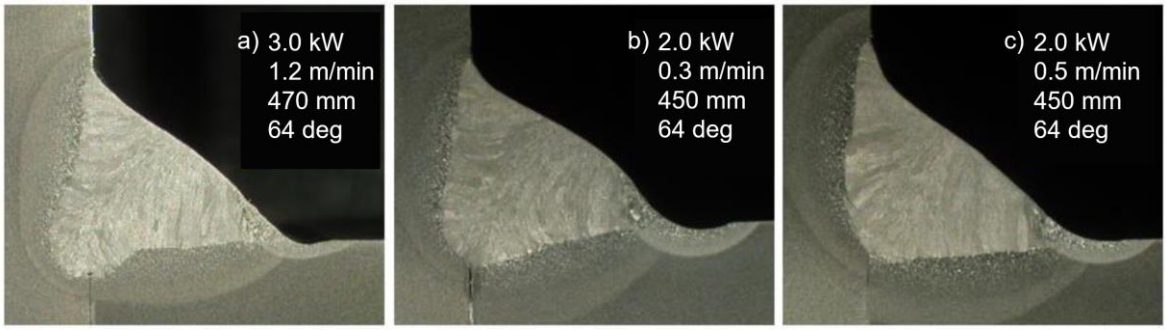

Fig. 12. Effect of travel speed of the laser beam and power on weld toe geometry after laser dressing.

Static tensile tests were carried out at room temperature and -40 °C, respectively. The results are shown in Fig. 13.

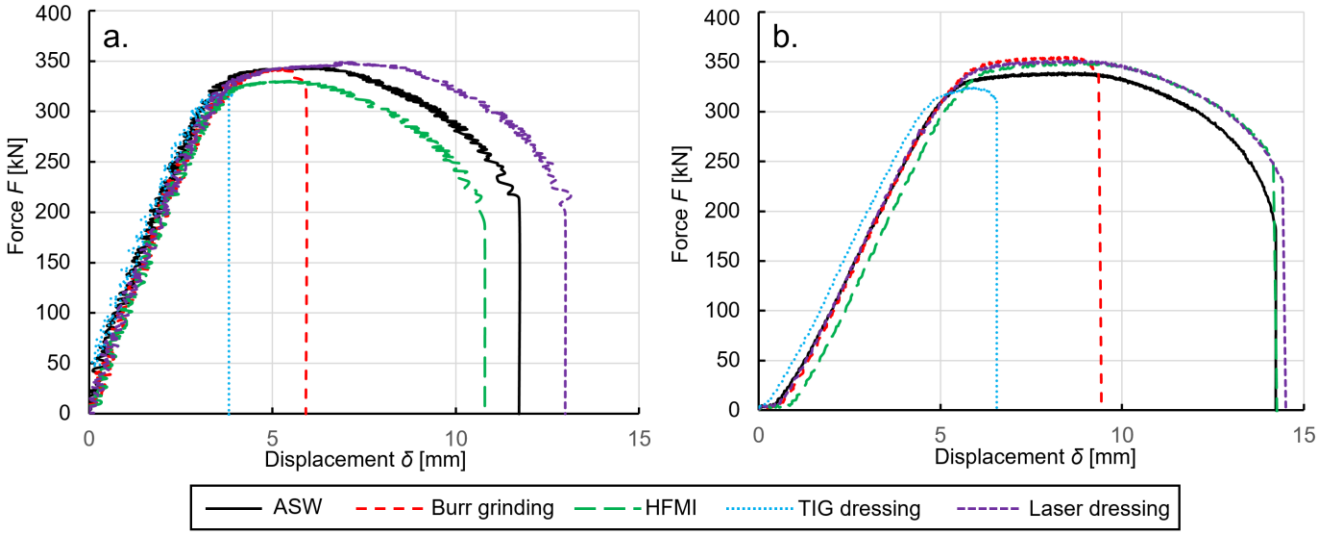

Fig. 13. Experimental load-displacement behaviors (a) at room temperature and (b) at -40 °C.

The results indicated that HFMI treatment and laser dressing have no effect on the ultimate capacity of the joint and the failures occurred outside the joint area at both test temperatures. Respectively, burr grinding, and particularly TIG dressing decreased the deformation capacity considerably as presented in Fig. 13. In both cases, the failure occurred at the treated weld toes, see Fig 14. Burr grinding decreases the net section, and the constraint effect by establishing a smooth transition area at weld toe.

Respectively, TIG dressing results in smooth transition similar to burr grinding, and causes detrimental softening through the plate thickness, see Fig. 14b. In addition, TIG dressing can also decrease net section depending on the TIG electrode alignment and welding parameters, see Fig. 14c where the net section has decreased due to TIG dressing. However, in the case of a thicker plate or one-sided attachment, the softening effect is not so pronounced. The test temperature seems to have no remarkable effect on the behavior of the post-treated joints.

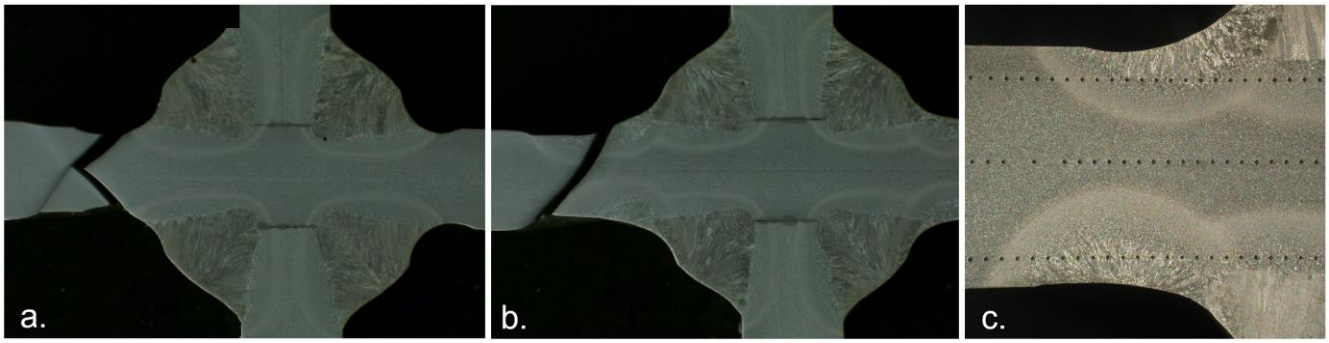

Fig. 14. Failures occurred at weld toe in a) burr grinded and b) TIG dressed joints. c) Net section reduction in a TIG dressed joint.

Laser dressing and HFMI treatment seem to be a promising improvement method because also current fatigue tests indicate improvement in fatigue performance [29]. However, laser dressing requires automatization and it is not thus always cost-efficient and feasible for fillet welded joints at the moment.

4 CONCLUSIONS

This paper investigated the numerical and experimental results obtained in the previous research work, focusing on the joints made of S960Q steel and consequently, the results and phenomena discussed in this study are valid for the quenched UHSSs. However, the phenomena can be applicable for other UHSSs, e.g. for quenched and tempered (QT) steels in some extent. Regarding particularly the quenched UHSSs, the following conclusions concerning the design of welded joints can be drawn:

- The softening at weld toe has a detrimental effect on the ultimate capacity of non-load carrying joints as well as load carrying joints and its applications need to be considered carefully.
- The deleterious effects of softening can be avoided by:
  a) proper design using constraint effect avoiding welds inclined with regards to direction of applied load, and
  b) suitable welding parameters.
- Heat input without supporting constraint effect, e.g. butt-welded joint with smooth transition and low weld reinforcement, is the worst case.
- Small throat thicknesses ($a = 4…5$ mm in GMAW processes) should be favored in order to increase the cooling rate, although it results in greater weld perimeters.
- The design of fillet welds with unequal leg lengths, i.e. asymmetric weld, eases fulfillment of geometrical requirements, and improves
  a) efficiency of joint in terms of joint capacity with respect to volume of weld
  b) fusion line strength
  c) fatigue strength
- Penetration should be favored instead of pure fillet welds, but the effect of softening of the penetrated area due to dilution should be considered.

- The secondary bending moment in welds cannot be ignored and the strength capacity of the joint loaded by a moment that causes tensile stresses in the weld root must be calculated according to elastic approach.
- In addition to HFMI treatment, weld toe treatment by laser dressing seems to be a promising process for static and fatigue strength improvement of welded joints.

ACKNOWLEDGEMENTS

The authors wish to thank SSAB, DIMECC Ltd. and the Finnish Funding Agency for Innovation (TEKES) for funding in the BSA (Breakthrough Steels and Applications) program that enabled this research work to be completed. Additionally, the authors express their gratitude to the IT Center for Science (CSC) for providing the licensing of software.

REFERENCES

1. EN 10149-2 (2013) Hot rolled flat products made of high yield strength steels for cold forming – Part 2: Technical delivery conditions for thermomechanically rolled steels.
2. EN 1993-1-8 (2005) Eurocode 3 - Design of steel structures - Part 1-8: Design of joints.
3. EN 1993-1-12 (2007) Eurocode 3 - Design of steel structures - Part 1-12: Additional rules for the extension of EN 1993 up to steel grades S700.
4. Björk T, Toivonen J, Nykänen T (2012) Capacity of fillet welded joints made of ultra high-strength steel. Weld World 56:71–84. doi: 10.1007/BF03321337
5. Björk T (2005) Ductility and ultimate strength of cold-formed rectangular hollow section joints at subzero temperatures. Doctoral dissertation. Lappeenranta University of Technology
6. EN 1011-1 (2009) Welding - Recommendations for welding of metallic materials - Part 1: General quidance for arc welding.
7. EN 1011-2 (2001) Welding - Recommendations for welding of metallic materials. Part 2: Arc welding of ferritic steels.
8. Karppi R, Leiviskä P, Laitinen R (2008) Developments in MAG-welding for ultra high strength steel; Optim 960 QC. In: Int. Symbosium From Weld. Fract. to Pipeline Technol. pp 1–20
9. Amraei M, Skriko T, Björk T, Zhao XL (2016) Plastic strain characteristics of butt-welded ultra-high strength steel (UHSS). Thin-Walled Struct 109:227–241. doi: 10.1016/j.tws.2016.09.024
10. Amraei M, Dabiri M, Björk T, Skriko T (2016) Effects of workshop fabrication processes on the deformation capacity of S960 ultra-high strength steel. J Manuf Sci Eng 138:121007.
11. Guo W, Crowther D, Francis JA, et al (2015) Microstructure and mechanical properties of laser welded S960 high strength steel. Mater Des 85:534–548. doi: 10.1016/j.matdes.2015.07.037
12. Siltanen J, Tihinen S, Kömi J (2015) Laser and laser gas-metal-arc hybrid welding of 960 MPa direct-quenched structural steel in a butt joint configuration. J Laser Appl 27:S29007. doi: 10.2351/1.4906386
13. Peltoniemi T (2016) The effect of stress concentration on the ultimate capacity of welded joints made of ultra-high strength steel. Master's thesis. Lappeenranta University of Technology
14. Porter D (2015) Weldable high-strength steels: Challenges and engineering applications. 68th IIW Annu. Assem. Int. Conf. High Strength Mater. - Challenges Appl.
15. Björk T, Nykänen T, Valkonen I (2017) On the critical plane of axially loaded plate structures made of ultra-high strength steel. Weld World 61:139–150. doi: 10.1007/s40194-016-0387-8
16. Penttilä T (2012) Static strength design of fillet welds with conventional methods and new improved design methods based on different boundary conditions (in Finnish). In: Proc. 11th Finnish Mech. Days. pp 169–176

17. Penttilä T (2013) Effects of different GMAW processes and parameters on behavior of transverse fillet welds made of ultra-high strength steels. Master's thesis. Lappeenranta University of Technology
18. Tousignant K, Packer J (2016) Fillet Welding to Hollow Structural Sections. IIW-document XV-1524-16.
19. EN ISO 5817 (2014) Welding. Fusion-welded joints in steel, nickel, titanium and their alloys (beam welding excluded). Quality levels for imperfections. 38.
20. Björk T, Penttilä T, Nykänen T (2014) Rotation capacity of fillet weld joints made of high-strength steel. Weld World 58:853–863. doi: 10.1007/s40194-014-0164-5
21. Pavlina EJ, Van Tyne CJ (2008) Correlation of Yield strength and Tensile strength with hardness for steels. J Mater Eng Perform 17:888–893. doi: 10.1007/s11665-008-9225-5
22. Anthes RJ, Köttgen VB, Seeger T (1993) Stress concentration factors for butt joints and double T-joints (in German). Schweißen und Scheiden 45:685–688.
23. Maddox SJ (1991) Fatigue strength of welded structures. Abington Publishing
24. Rasche C, Kuhlmann U (2010) The load bearing capacity of fillet welded connections of high strength steels. In: IABSE Symp. pp 71–78
25. Rasche C, Kuhlmann U (2012) Load bearing capacity of fillet welded connections of high strength steel (in German). Stahlbau 81:889–897. doi: 10.1002/stab.201201628
26. Tuominen N, Björk T, Ahola A (2017) Effect of bending moment on capacity of fillet weld. 16th Int. Symp. Tubul. Struct. ISTS16
27. Tuominen N, Björk T, Litmanen J (2016) Effect of secondary moment on the strength of weld (in Finnish). J Struct Mech 49:237–251.
28. Haajanen M (2017) Effect of post-weld treatment on the static strength of ultra-high strength steel (in Finnish). Bachelor's thesis. Lappeenranta University of Technology
29. Skriko T (2018) Dependence of manufacturing parameters on the performance quality of welded joints made of direct quenched ultra-high-strength steel. Doctoral Dissertation. Lappeenranta University of Technology. Under work, submitted for preliminary examination.